We are IntechOpen, the world's leading publisher of Open Access books Built by scientists, for scientists

4,800
Open access books available

122,000
International authors and editors

135M
Downloads

Our authors are among the

154
Countries delivered to

TOP 1%
most cited scientists

12.2%
Contributors from top 500 universities

CLARIVATE ANALYTICS BOOK CITATION INDEX INDEXED

WEB OF SCIENCE™

Selection of our books indexed in the Book Citation Index in Web of Science™ Core Collection (BKCI)

Interested in publishing with us?
Contact book.department@intechopen.com

Numbers displayed above are based on latest data collected.
For more information visit www.intechopen.com

Chapter 11

Neurovascular and Neurometabolic Uncoupling in the Visual Cortex

Ai-Ling Lin, Jia-Hong Gao and Peter T. Fox

Additional information is available at the end of the chapter

http://dx.doi.org/10.5772/51074

1. Introduction

The quest to understand the functional organization of the brain by assessing changes in brain circulation has occupied scientists for more than a century. Significant increases in cerebral blood flow (CBF) accompany brain activity. The direct relationship between CBF and brain activity has been known since 1881(1). For more than a century, neuroscientists have assumed that increased metabolic demands in response to brain activation drive the elevation of CBF. Researchers could not investigate the hypothesis further until the 1980s, with the development of positron emission tomography (PET), a noninvasive imaging method to measure hemodynamic and metabolic changes in response to task-induced brain activation. Using PET and visual stimulation, Fox and colleagues (2) found that CBF increases were linearly coupled with neuronal activity as expected; however, changes in the cerebral metabolic rate of oxygen ($CMRO_2$) were significantly lower than that of CBF. The CBF–$CMRO_2$ "uncoupling" phenomenon therefore contradicts the early hypothesis.

The "uncoupling" discovery not only reshaped our understanding of the flow–metabolism interaction in response to brain activation but also led to the discovery of blood oxygenation level–dependent (BOLD) functional magnetic resonance imaging (fMRI) in the 1990s (3, 4). Further, the discovery evoked heated debate on physiological interpretations—for example, whether oxidative metabolism or glycolysis meets the energy demand during brain activation, and whether oxygen demand or some other mechanism mediates increases in CBF. In this chapter, we review the historical events that led to using PET to discover the neurovascular and neurometabolic "uncoupling"; the invention of BOLD fMRI techniques; and the development of physiological hypotheses to resolve the "uncoupling" mystery in the visual cortex.

2. Neurovascular and neurometabolic uncoupling in the visual cortex

2.1. Brain Activity vs. Cerebral Blood Flow

Italian physiologist Angelo Mosso first observed the relationship between CBF and neuronal activity in the late nineteenth century (1). Mosso invented an apparatus to simultaneously compare human intracranial pressure changes measured through a traumatic skull injury with pressure changes in the forearm or foot (Figure 1). Using this approach, he investigated particular cerebral hemodynamic patterns during emotional and cognitive experiences. His most famous report was the case of Michele Bertino, a 37-year-old farmer who had a large fracture to the skull (1). The fractured bone pieces were removed and the cerebral mass was exposed through a 2-cm bone breach in the right frontal region. Mosso recorded changes in brain volume related to CBF through a button fixed to the wooden cupola with a sheet of gutta-percha resting on Bertino's exposed dura mater and connected to a screw on the recording drum (Figure 2A).

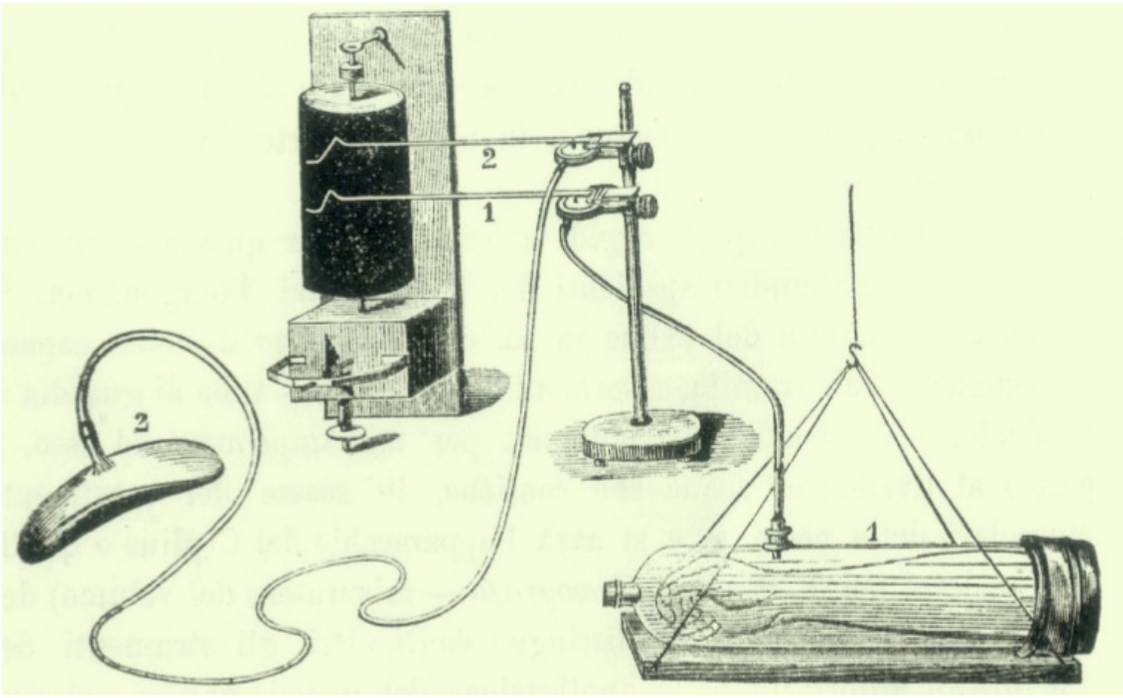

Figure 1. Mosso's devices for recording the blood volumes in arm and brain. 1, Forearm pulsation recording; 2, brain pulsation recording. Source: (5).

When the blood volume in the brain changed, the pulsation of the brain increased, increasing the pressure on the button and on the screw, thus compressing the air inside the drum. Changes in air compression were transmitted to a second recording drum and then written on a rotating cylinder. When Mosso asked Bertino to multiply 8 × 12, the pulsations of the brain increased within a few seconds after the request—but pulsations in the forearm did not. Similarly, when Mosso asked whether the chiming of the local church bell reminded Bertino that he had forgotten his midday prayers, Bertino said yes, and his brain pulsated again (Figure 2B).

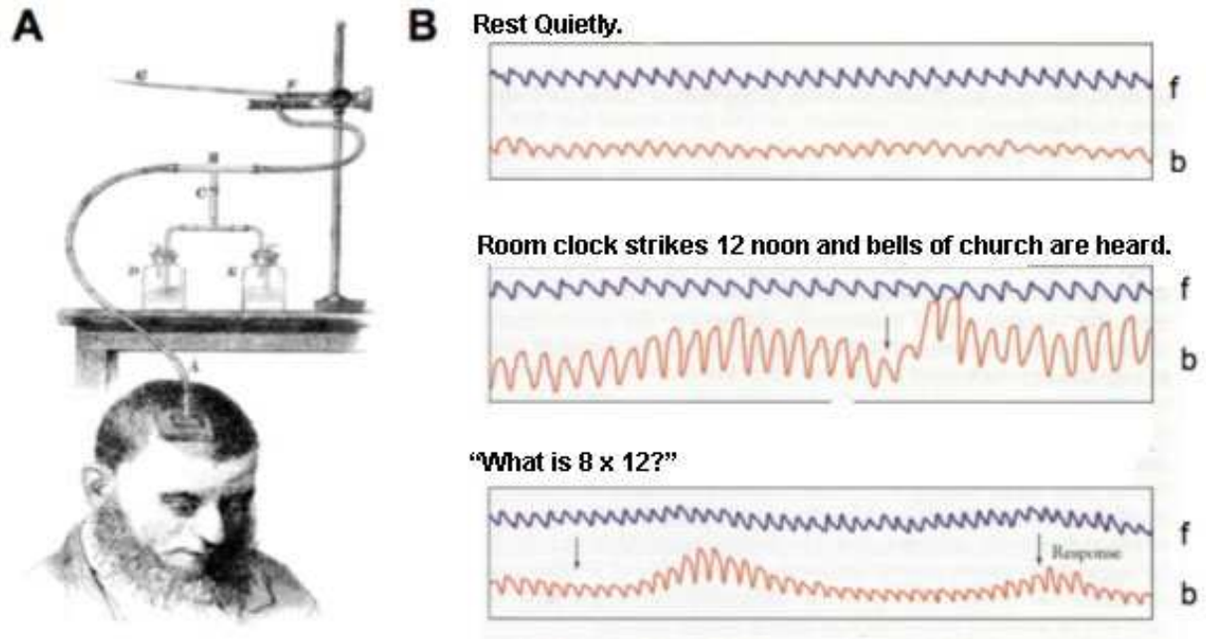

Figure 2. **(A)** The apparatus Mosso used to record Bertino's brain pulsations. **(B)** Mosso's recordings, taken from the forearm (f) and the brain (b), show stronger brain pulsations after events (marked by the arrows) that stimulated brain activity. Source: (1).

These studies suggested that measuring CBF might be an important way to assess brain function during mental activity. Roy and Sherrington, two distinguished British physiologists, further characterized the relationship between brain function and CBF (6). They attributed task-induced vasodilation to an increased demand for cerebral metabolism in response to neuronal activity. They stated, "the chemical products of cerebral metabolism contained in the lymph which bathes the walls of the arterioles of the brain can cause variations of the caliber of the cerebral vessels: that in this re-action the brain possesses an intrinsic mechanism by which its vascular supply can be varied locally in correspondence with local variations of functional activity". This statement implies that cerebral functional activity, energy metabolism, and blood flow are closely related. Researchers have interpreted the Roy–Sherrington principle to mean that CBF changes reflect a tight coupling between cellular energy requirements and vascular delivery of glucose and oxygen.

Over the past century, the visual cortex has made significant contributions to the evolving investigations of the Roy–Sherrington principle. The first report of the close relationship between CBF and neuronal activation in the visual cortex was in 1928 by Dr. John Fulton, of the neurosurgery clinic at the Peter Bent Brigham Hospital in Boston (7). Fulton's patient had suffered a gradual loss of vision due to a collection of congenitally abnormal blood vessels serving his visual cortex. Unlike the smooth, silent blood flow in normal blood vessels, the blood flow through these abnormal vessels was turbulent and created a brief rushing sound with each heartbeat. The patient could hear this sound, as could his physicians when they listened with their stethoscope through a defect in the skull (Figure 3A). The sound increased whenever the patient opened his eyes and especially when he read a newspaper (Figure 3B).

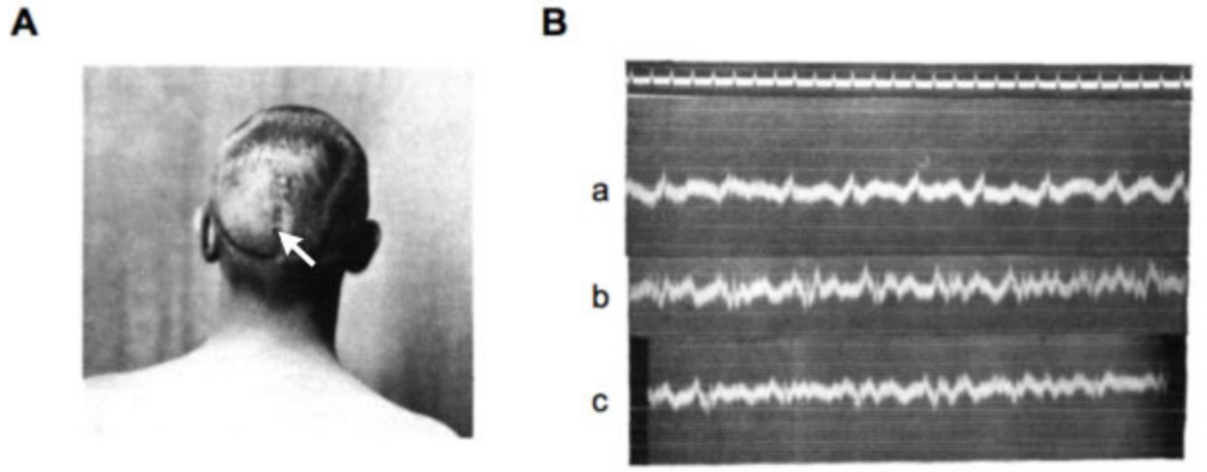

Figure 3. **(A)** Patient 3 weeks after operation, showing the region explored. The arrow indicates the point of maximum intensity of the bruit. This overlies the region of greatest vascularity of the angioma. **(B)** Typical electrophonograms of bruit **(a)**, after 10 minutes' rest in a darkened room; **(b)**, after 2 minutes' reading of small print illuminated by a single 40-watt tungsten bulb at 5 feet; **(c)**, 3 minutes later, after 2.5 minutes' rest in a darkened room. Time above: 0–2 sec. Source: (7).

The correlation between CBF changes in a specific sensory system (visual system) during mental activity (reading) was remarkable. However, the full importance of this work was not appreciated until the development of accurate techniques to measure CBF and brain metabolism in laboratory animals and in humans.

The development of positron emission tomography (PET) in the 1960s further advanced the field of research. PET is a nuclear medicine imaging technique that produces a three-dimensional, in vivo image of functional processes in the body. Using ^{15}O-labeled water (i.e., $H_2{}^{15}O$; half-life = 123 sec) as a freely diffusible tracer, PET can measure CBF in less than 1 min. With these techniques, Fox and Raichle (8) revisited the task-induced neurovascular coupling in the human visual cortex in vivo. They measured CBF changes with a visual system that delivered full-field flashes of fixed wavelength, luminance, and duration over frequencies from 1 to 60 Hz (Figure 4A). For the first time, noninvasive neuroimaging showed localized CBF changes in the human visual cortex in response to neuronal activation (Figure 4, B to D). Knowing that the time for full recovery of the visual-evoked potential was approximately 125 msec and that $H_2{}^{15}O$ PET measurements integrated over 40 sec, Fox and colleagues reasoned that the CBF response should be linear at least up to a repetition rate of 8 Hz (i.e., 1/0.125 sec; the stimulation is not effective for stimulus frequency >8 Hz). The findings were in excellent agreement with their hypothesis: CBF rose linearly with stimulus rate ($r = 0.886$; $p < 0.0005$), peaking at 7.8 Hz (Figure 5, A and B). Response locations also were tightly grouped. The rate–response function soon was replicated and extended by using a reversing checkerboard, constant-luminance stimulus (9). The pioneer works by Fox and colleagues were significant in two aspects: they were the first studies to show CBF in response to visual stimulation in conscious adult humans, and they confirmed that CBF is linear coupled with neuronal activity till it reaches the maximal visual-evoked potential.

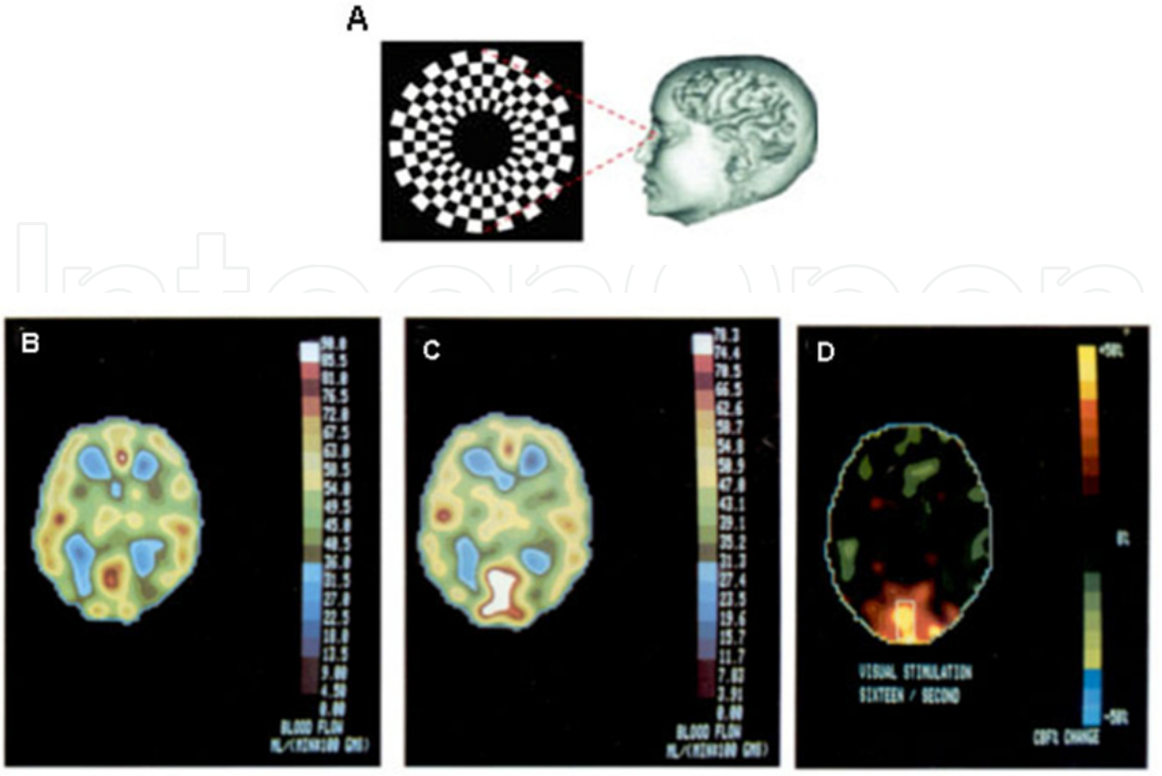

Figure 4. **(A)** Checkerboard stimulation. **(B)** CBF image during the initial unstimulated state. **(C)** CBF image during 16-Hz photic stimulation. **(D)** CBF image of panel C (16 Hz) versus panel B (unstimulated). The position and configuration of the regional CBF response elicited by repetitive patterned-flash stimuli are illustrated. Source: (8).

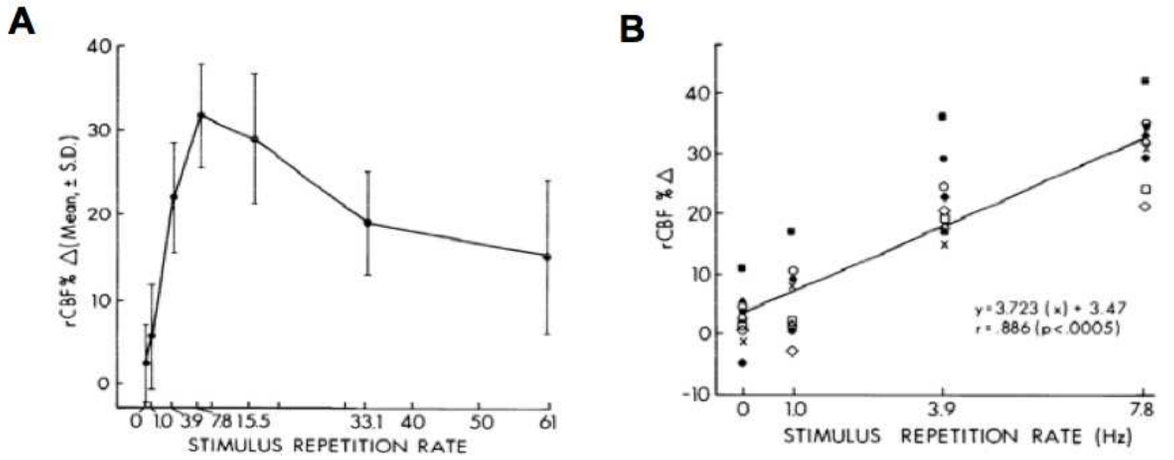

Figure 5. **(A)** Photic stimulation caused a selective regional CBF (rCBF) increase in the striate cortex up to a maximum response at 7.8 Hz. The rCBF declined with frequency increases beyond 7.8 Hz but remained above the unstimulated state. Each point and error bar represent the mean ± SD at each stimulus frequency. rCBF response is expressed as the percent change from the initial unstimulated scan. **(B)** Striate cortex percent change in rCBF from the initial unstimulated state, varied as a linear function of stimulus frequency between 0 and 7.8 Hz. The function of the linear regression is given and the regression line plotted. Source: (8).

2.2. Discovery of the neurovascular and neurometabolic uncoupling

With these powerful tools in hand, Fox and colleagues took a further step to test the Roy–Sherrington principle, that is, to determine whether increased metabolic demands (i.e., glucose and oxygen consumption) in response to neuronal activity drove the task-evoked CBF changes. At first, researchers rationally assumed that cerebral metabolic rate of glucose (CMR_{Glc}) and oxygen ($CMRO_2$) would increase proportionally with the increased CBF and neuronal activity because neurons account for most of the energy consumption during brain activation through ATP generated by oxidative phosphorylation of glucose. In addition to CBF, they measured CMR_{Glc} by using ^{18}F-labeled 2-fluoro-2-deoxy-D-glucose (^{18}FDG) and $CMRO_2$ by using ^{15}O-labeled oxygen ($^{15}O_2$). Again, using visual stimulation as a paradigm, Fox and colleagues used PET to simultaneously measure the task-induced changes in CBF, CMR_{Glc}, and $CMRO_2$ in the activated human cortex. As expected, task performance reliably elicited large, highly focal increases in CBF (2) and CMR_{Glc} (2, 10) (Figure 6A). The observed increases in CBF and CMR_{Glc} were similar in magnitude, typically 30%–50%.

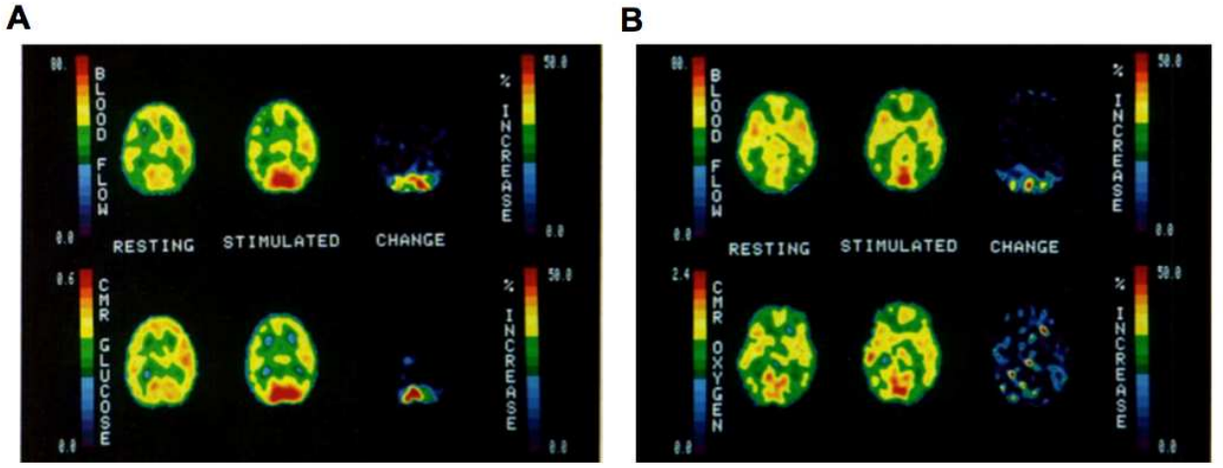

Figure 6. **(A)** Glucose metabolic rate (lower row) and blood flow (upper row) were closely coupled throughout the brain both at rest and during visual stimulation. Phasic neural activation (visual stimulation) increased regional glucose uptake and blood flow by a similar amount (51% and 50%, respectively). **(B)** The metabolic rate of oxygen (lower row) and blood flow (upper row) were closely coupled throughout the brain at rest. Visual stimulation, however, increased regional oxygen consumption minimally (5%) while markedly increasing blood flow (50%). Source: (2).

However, to their surprise, Fox and colleagues (2) observed that task-induced increases in $CMRO_2$ (5%) were much lower than those in CBF or CMR_{Glc} (Figure 6B). The $CMRO_2$ shortfall during focal neuronal activation, in fact, caused a local oxygen surplus, with the oxygen extraction fraction falling from a resting value of ~40% to a task-state value of ~20%. These findings contradicted the Roy–Sherrington hypothesis.

Because either oxidative or nonoxidative (i.e., lactate producing) pathways can metabolize glucose and because the increase of $CMRO_2$ was minimal, Fox and colleagues suggested that (i) glucose is predominately metabolized by anaerobic glycolysis; (ii) the energy demand associated with neuronal activation is small (as opposed to resting-state demand), and

glycolysis alone may provide the energy needed for the transient changes in brain activity; and (iii) factors other than oxidative metabolism and total energy demand must regulate CBF response.

Using ^{1}H nuclear magnetic resonance spectroscopy (MRS), a method that exploits the magnetic properties of metabolites, Prichard and colleagues observed that tissue lactate concentration [Lac] significantly increases during visual stimulation (Figure 7, A and B). The observation confirmed that the stimulus-evoked increase in glucose consumption observed with PET is at least partially nonoxidative (11, 12).

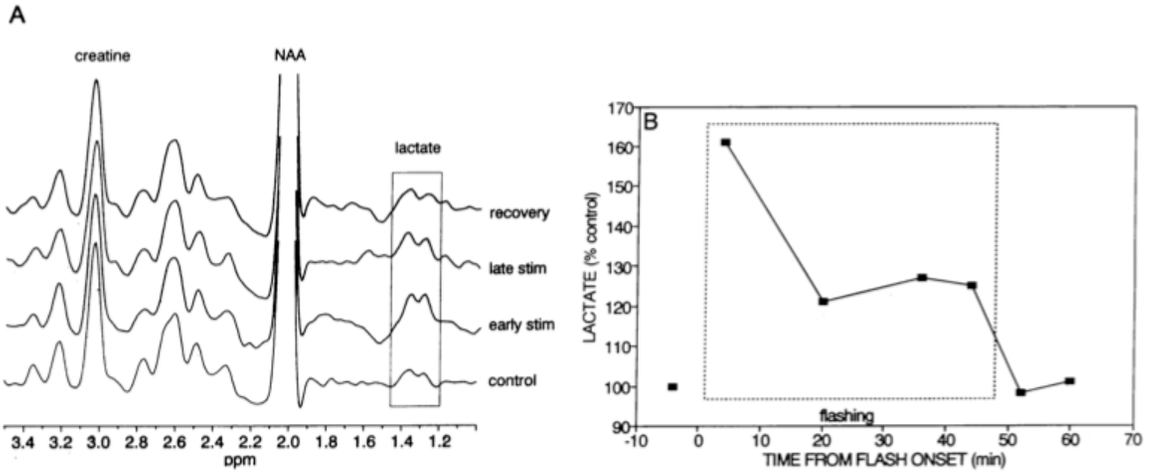

Figure 7. (A) ^{1}H spectra from 13 cc of human visual cortex before, during, and after photic stimulation (stim) by red dot grids flashing at 16 Hz in front of each eye. The frequency axis is in ppm and was set from the prominent resonance of *N*-acetylaspartate (NAA) at 2.02 ppm. The shaded area highlights the lactate methyl proton resonance at 1.33 ppm, with its characteristic 7-Hz splitting. The creatine resonance at 3.04 ppm is the total signal from methyl protons of phosphocreatine and creatine. **(B)** Time course of the experiment illustrated in panel A, with intensities of the lactate resonance plotted as a percentage of its control intensity. Source: (11).

Later studies further identified that CBF–$CMRO_2$ uncoupling also depended on rate and duration (13, 14). Using graded visual stimulation, Vafaee and Gjedde (13) found that the percent fractional changes (%Δ) in CBF peaked at 8 Hz, similar to the finding of Fox and colleagues, whereas %Δ$CMRO_2$ reached a maximum at 4 Hz (Figure 8). With prolonged visual stimulation (25 min), Mintun and colleagues (14) found that after 1 min of stimulation, $CMRO_2$ increased only 4.7% compared with baseline and CBF increased 40.7% (Figure 9, A and B). However, after 25 min of stimulation, the increase in $CMRO_2$ compared with baseline was 15.0%, having tripled from that measured at 1 min (Figure 9B). CBF decreased to 37.1% after 1 min of visual stimulation and then returned almost to baseline values after 25 min of activation (Figure 9A). These two studies further supported the Fox group's argument that factors other than oxidative metabolism regulate CBF response.

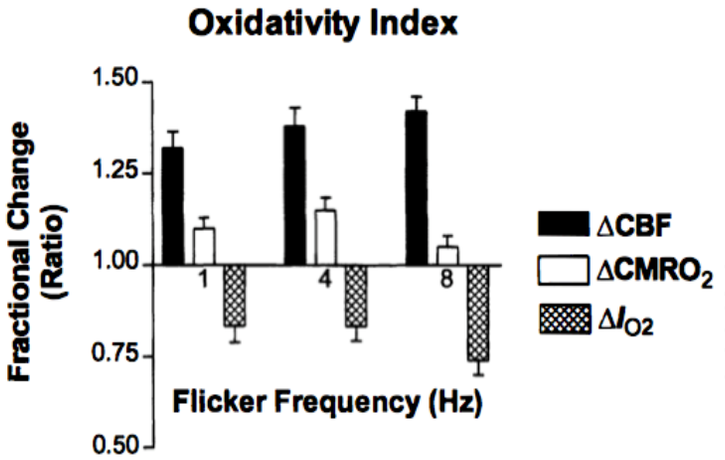

Figure 8. Percent changes of CBF, $CMRO_2$, and $CMRO_2$:CBF ratio index (I_{O2}) in the primary visual cortex as a function of checkerboard contrast reversal rate. Note maximum I_{O2} change at 8 Hz. Source: (13).

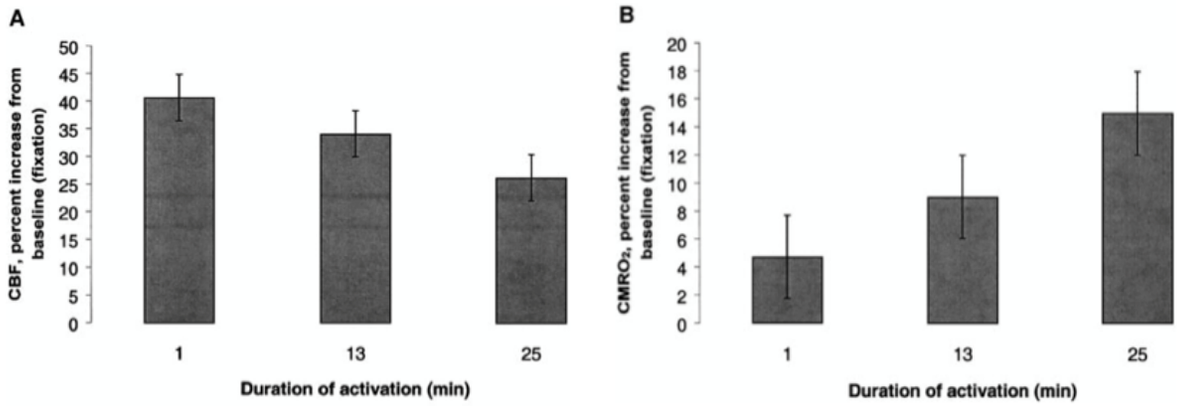

Figure 9. Effects of continuous visual stimulation on rCBF **(A)** and $CMRO_2$ **(B)**. Data shown represent the mean percent change from baseline (fixation) in seven subjects. CBF increased significantly early after the onset of visual stimulation and then had a nonsignificant tendency to decrease. Initial increase in $CMRO_2$ was small (4.7%); however, it tripled during continued stimulation and reached significant levels (15%, $p < 0.01$) at 25 min. Source: (14).

2.3. Discovery of functional magnetic resonance imaging

The CBF–$CMRO_2$ uncoupling phenomenon led to the discovery of functional magnetic resonance imaging (fMRI), known as the blood oxygenation level–dependent (BOLD) contrast, by Ogawa and others (3, 4). The physical effect is based on the magnetic property difference between deoxyhemoglobin (dHb; i.e., hemoglobin not bound with oxygen) and oxyhemoglobin (Hb; i.e., hemoglobin that binds with oxygen). Magnetic fields can weakly repel Hb, which is diamagnetic, whereas they can attract dHb, which is paramagnetic (which makes the magnetic field less uniform and thus decreases MR signal). The dramatic increases in CBF, relative to $CMRO_2$, bring in excess Hb (relative to dHb) to the venous blood, which causes measurable changes in the MRI signal (BOLD contrast).

In 1992, Kwong et al. used the BOLD contrast to study activation in the human visual cortex (15). During stimulation, they detected local increases in signal intensity in the medial-posterior regions of the occipital lobes along the calcarine fissures (Figure 10A). Their results independently confirm PET observations that little or no increase in tissue oxygen consumption accompanies activation-induced changes in blood flow and volume (2). They also observed rate-dependent increases of BOLD signal, peaking at 8 Hz, consistent with the PET observations for CBF (8) (Figure 10B).

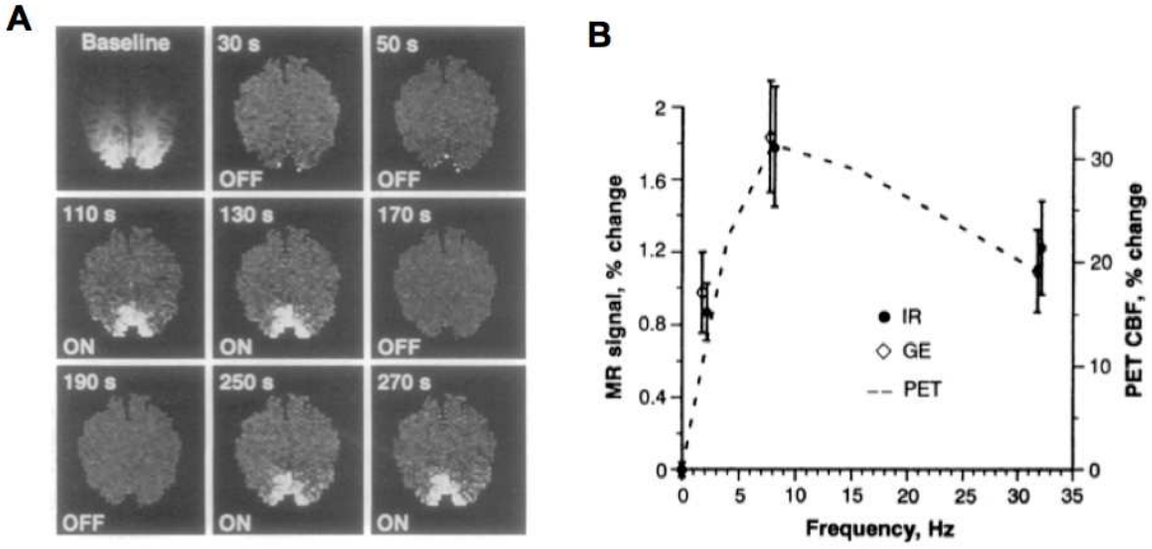

Figure 10. **(A)** Noninvasive, real-time MRI mapping of V1 activation during visual stimulation. A baseline image acquired during darkness (upper left) was subtracted from subsequent images. Eight of these subtraction images are displayed, chosen when the image intensities reached a steady-state signal level, during darkness (OFF) and during 8-Hz photic stimulation (ON). **(B)** BOLD signal as a function of the frequency of light stimulus (0 Hz = darkness). Signal response is expressed as percent change from baseline unstimulated level. The largest observed response occurred at 8 Hz. For comparison with data from Fox and colleagues, CBF percent changes obtained by PET with the same stimulation paradigm at 0, 1, 4, 8, 16, and 32 Hz are superimposed on the MR data. Source: (15).

Using BOLD signal, Davis and colleagues developed mathematical modeling to determine task-induced changes in $CMRO_2$. By combining with MRI-based CBF measurement using arterial spin labeling techniques (16), researchers can compute relative $CMRO_2$ changes ($rCMRO_2$) by measuring evoked-induced changes in BOLD and CBF and basal BOLD relaxation rate (M value) (Eq. [1]). Consistent with the PET-based measurement, $CMRO_2$ changes (16%) were much smaller than CBF changes (45%) during visual stimulation (17).

$$\mathrm{rCMRO}_2(t) = CBF(t)^{1-\alpha/\beta}\left(1-\frac{BOLD(t)-1}{M}\right)^{1/\beta} \quad (1)$$

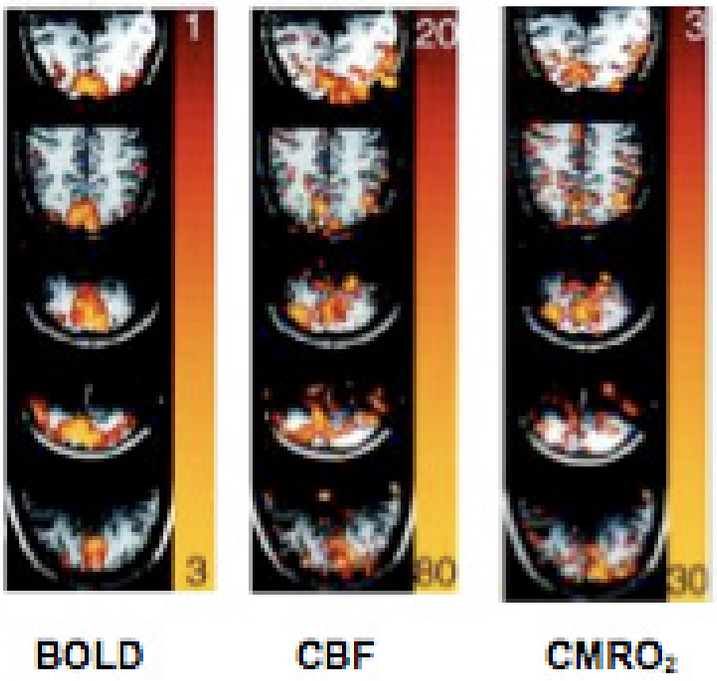

Figure 11. The left column shows BOLD task activation responses as color overlays: colors represent signal increases from 1% (red) to 3% (yellow). The center column shows CBF task activation increasing from 20% to 80%. The rightmost column shows $rCMRO_2$ for each subject, from 3% to 30%. All subjects show a confluent patch of increased $rCMRO_2$ in the visual cortex, averaging from 13% to 19%. Some peaks reach up to 30% increase in metabolism, corresponding to peaks of blood flow up to 70%. Source: (17).

Taken together, the PET and fMRI results showed that the increases in CBF and $CMRO_2$ during visual stimulation are uncoupled, summarized as follows (18): Compared with viewing a blank screen, visual stimulation produces marked changes in activity in visual areas of the brain, as shown in the PET images (from small increase, blue, to major increase, red; Figure 12). Increases in both blood flow and glucose use in the visual cortex could be observed, without similar increases in oxygen use. As a result, local oxygen availability increases because of the increased supply of oxygen from flowing blood that exceeds the increased local demand for oxygen, which forms the fMRI BOLD contrast.

2.4. Bioenergetics in the Visual Cortex

Despite the agreement across imaging modalities in the observation of CBF–$CMRO_2$ uncoupling, the physiological interpretation for this phenomenon has been controversial. Two major debates were whether oxidative metabolism regulates CBF and whether oxidative metabolism or nonoxidative glycolysis meets the energy demands for neuronal activity.

In contrast to the suggestion of Fox and colleagues that oxygen demand did not regulate CBF increases and that glycolysis can meet the neuronal energy requirements, others argued

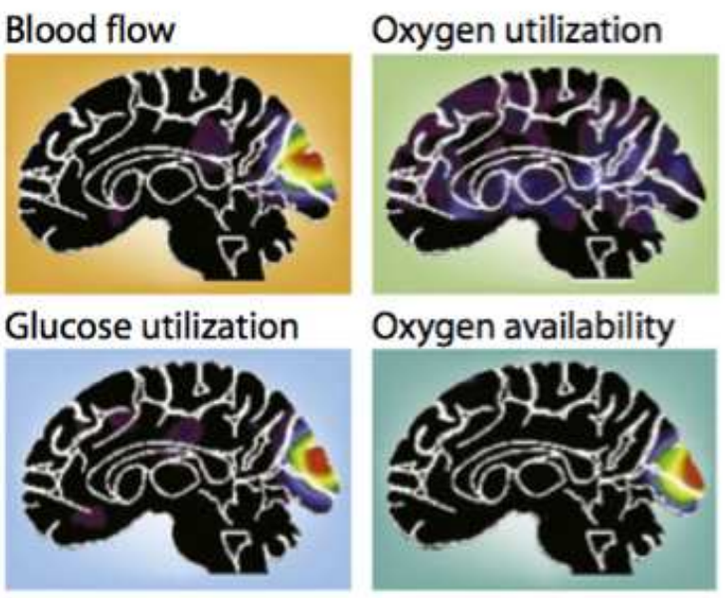

Figure 12. Visual stimulation produces marked changes in activity in visual areas of the brain. Blood flow, glucose utilization, and oxygen availability significantly increase, but the change of the oxygen utilization is minimal. Source: (18).

that significant increases of CBF were needed to facilitate oxygen delivery and that predominately oxidative metabolism should meet energy demands (19). To clarify whether oxidative metabolism or glycolysis regulates CBF and energy demands, Lin and colleagues (20) performed a concurrent fMRI and ^{1}H MRS study using graded visual stimulation (4, 8, and 16 Hz). They used fMRI to determine %ΔCBF and %Δ$CMRO_2$ and used ^{1}H MRS to determine %Δ[Lac].

Findings for %ΔCBF, %Δ$CMRO_2$, and %Δ[Lac] varied with frequency, with %ΔCBF and %Δ[Lac] peaking at 8 Hz, whereas %Δ$CMRO_2$ reached a maximum at 4 Hz (Figure 13, A and B). The magnitudes of %ΔCBF (57.1%–65.1%) and %Δ[Lac] (31.3%–50.0%) were much larger than that of %Δ$CMRO_2$ (12.2%–17.0%). As a result, %ΔCBF was tightly coupled with lactate production rate (Figure 14A) but negatively correlated with %Δ$CMRO_2$ (Figure 14B).

ATP production (J_{ATP}) was calculated, using a stoichiometric equation, from the determined %Δ$CMRO_2$ and lactate production rate. J_{ATP} was not significantly different among the three stimulus frequencies, and the increment was smaller (12%–17%) than the baseline (Rest) state. Further, oxidative metabolism predominately contributed to J_{ATP} and linearly correlated with %Δ$CMRO_2$ (Figure 14C and Figure 15).

Taken together, the major findings from the study were as follows: (i) Increases in oxygen metabolism and energy demand of task-induced neuronal activation were small (12%–17%); (ii) oxidative (indexed by $CMRO_2$) and nonoxidative (indexed by lactate production) metabolism coexisted during visual stimulation; and (iii) CBF increase was much larger (52%–65%) than the increase in energy demand and highly correlated with lactate production, but not with $CMRO_2$. In response to the two main debated questions mentioned

above, Lin et al's observations supported that (i) anaerobic glycolysis, rather than oxygen demand, drives CBF response to neuronal activity, and (ii) energy demand is predominately met through the oxidative metabolic pathway even though the $CMRO_2$ increases are much lower than those of [Lac] (19, 21, 22).

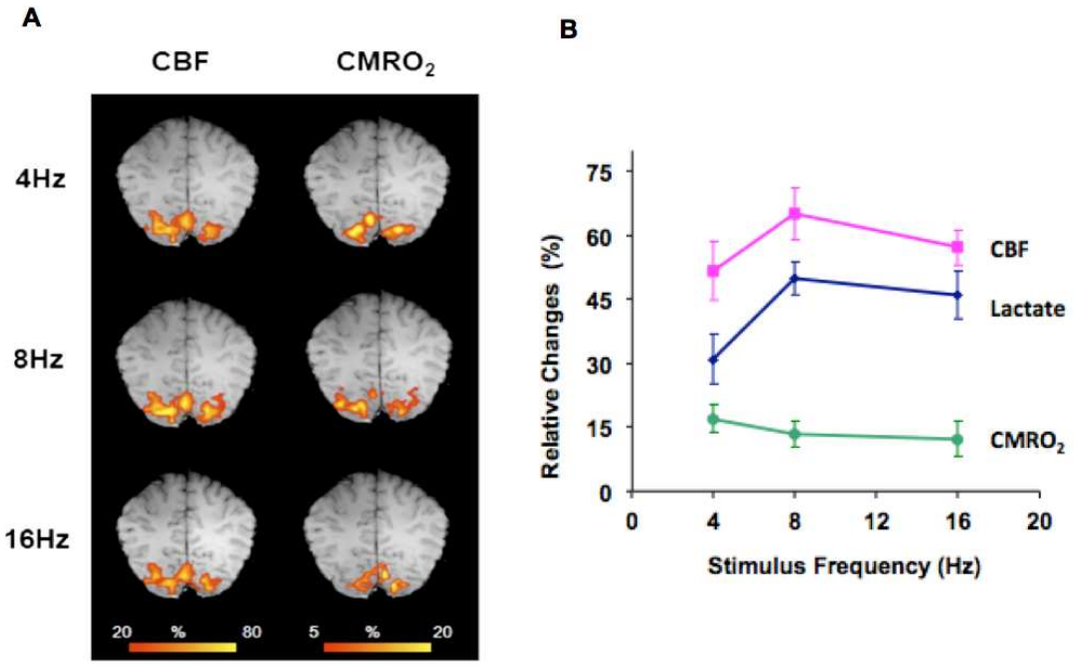

Figure 13. **(A)** Location and magnitude of %ΔCBF and %ΔCMRO2 in the primary visual cortex during 4-, 8-, and 16-Hz visual stimulation. **(B)** Magnitude of %ΔCBF, %Δ[Lac], and %ΔCMRO2 in the primary visual cortex during 4-, 8-, and 16-Hz visual stimulation. Source: (20).

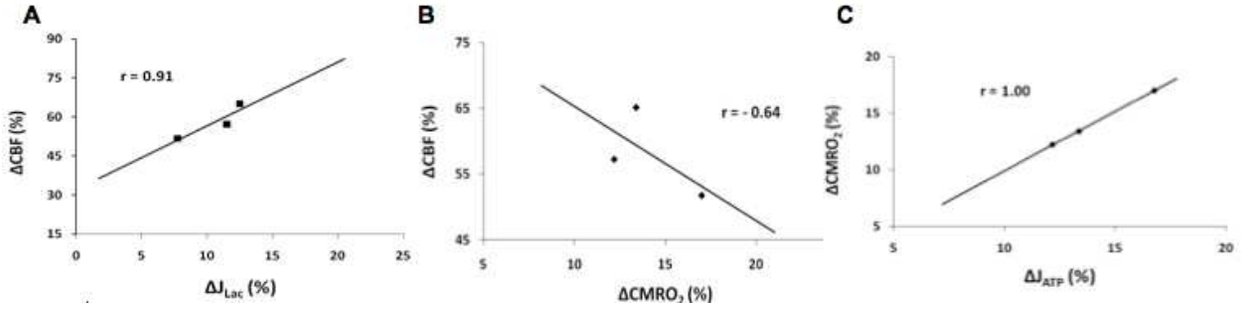

Figure 14. **(A)** CBF–lactate coupling. Significant correlation existed between %ΔCBF and $\%\Delta J_{Lac}$ at the three visual stimulation rates ($r = 0.91$; $p < 0.001$). **(B)** CBF–$CMRO_2$ coupling. Negative correlation existed between %ΔCBF and %ΔCMRO2 at the three visual stimulation rates ($r = –0.64$; $p = 0.024$). **(C)** $CMRO_2$–ATP coupling. Significant correlation existed between %ΔCMRO2 and $\%\Delta J_{ATP}$ at the three visual stimulation rates ($r = 1.00$; $p < 0.001$). Source: (20).

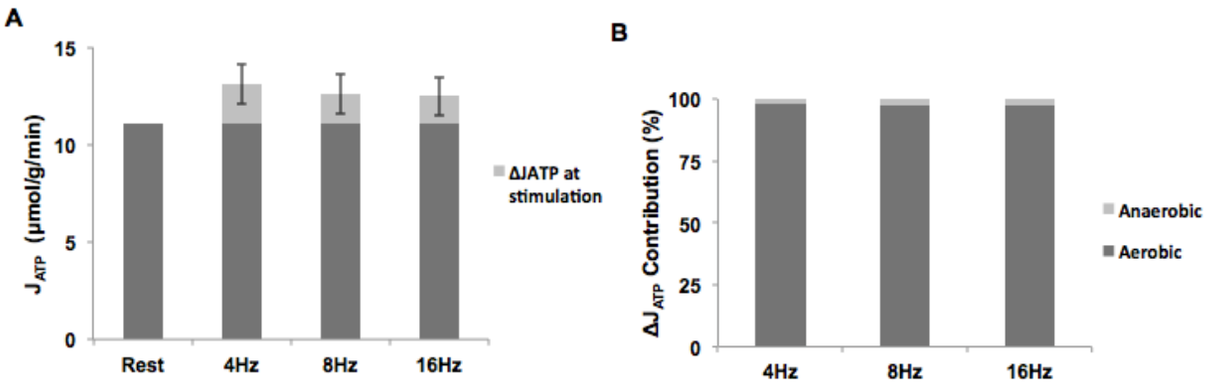

Figure 15. **(A)** J_{ATP} at rest and the three levels of visual stimulation. The J_{ATP} values during activation are independent of stimulus rate. The increments at activation are smaller (1.4–2.0 μmol/g/min) than the rest value (11.1 μmol/g/min). **(B)** Aerobic and anaerobic relative contributions (%) to ΔJ_{ATP}. The ΔJ_{ATP} at the three stimulation rates is due predominately to aerobic metabolism (~98%, including both neuronal and astrocytic contributions). Source: (20).

2.5. Astrocyte–Neuron Lactate Shuttle (ANLS) Model

The collective evidence from the functional imaging literature (PET, fMRI, and MRS) has forced the development of alternatives to the Roy–Sherrington hypothesis. Of these, the astrocyte–neuron lactate shuttle (ANLS) model (Figure 16) is the most conceptually evolved and widely accepted (23, 24). The ANLS model posits a cooperation between neurons and astrocytes in meeting the activation-induced needs both for energy production and for neurotransmitter production. Upon neuronal firing, both neurons and astrocytes take up glucose. Astrocytes take up most of the glucose, and neurons take up the rest. Though the level of glucose metabolism in neurons is low, the process is entirely aerobic to support neurotransmission (25, 26). The level of astrocytic glucose consumption, however, is high but much less energetically efficient because it is predominately anaerobic. Astrocytic glycolysis (2 ATP) is used to support Na^+/K^+ ion pumping and glutamate (Glu)–glutamine (Gln) conversion. Lactate generated by astrocytic glycolysis is eventually transported to neurons as fuel, but with some loss into the circulation, which increases hyperemia (26, 27). The ANLS hypothesis implies that (i) oxygen demand does not drive increases in CMR_{Glc}, which serve other purposes such as astrocyte-mediated neurotransmitter recycling; (ii) task-induced oxygen demand is small; and (iii) factors other than oxidative metabolism regulate CBF increases.

The three findings that Lin and colleagues reported, described above, were in good agreement with the ANLS hypothesis. The first finding (small $CMRO_2$ increase) was in line with the ANLS implication that the energy demands of acute, transient increases in neuronal activity are small (~15% increase in $CMRO_2$; at most, 30%). Oxidative metabolism should increase as neuronal activation continues because neurons eventually take up astrocytic lactate into the tricarboxylic acid cycle as a fuel substrate. In support of this formulation, prolonged visual stimulation (>20 min) can induce gradually rising levels of $CMRO_2$ and gradually decreasing CMR_{Glc}, J_{Lac}, and CBF under high-frequency stimulation

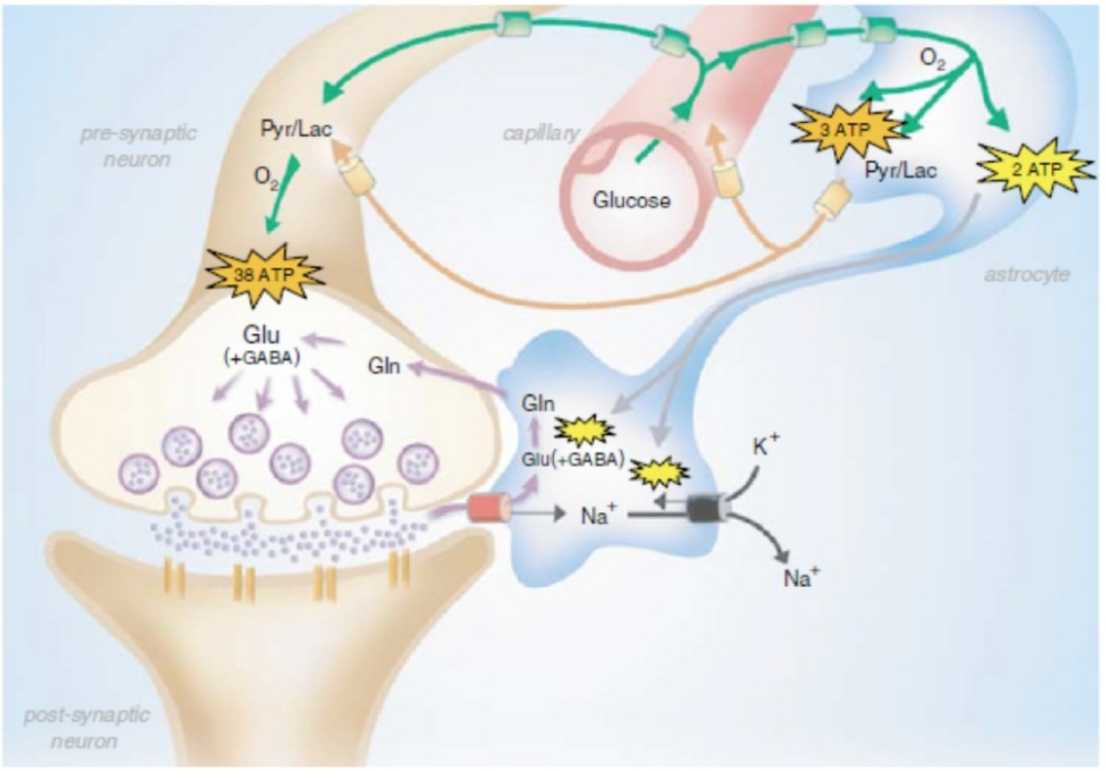

Figure 16. The Astrocyte-neuron lactate shuttle (ANLS) model. Glucose (green arrows) is delivered via the capillaries to both neurons (beige) and astrocytes (blue). In neurons, glucose consumption is predominately oxidative, generating 38 ATP at a glucose oxidation rate of 1.00 μmol/g/min. In astrocytes, glucose consumption is both oxidative and nonoxidative, generating 3 ATP oxidatively and 2 ATP nonoxidatively (at a glucose oxidation rate of 1.00 μmol/g/min). The energy from nonoxidative metabolism is used to convert glutamate to glutamine, the predominant excitatory neurotransmitter. Neurons take up the lactate that glycolysis generates to fuel further glucose oxidation. A small amount of lactate will efflux to the capillaries and thus increase cerebral blood flow (CBF). Source: (26).

(e.g., 8 Hz) (11, 14, 28-30). Consequently, %ΔCBF and %ΔCMRO$_2$ were recoupled as stimulation continued (14, 28), as mentioned in section 2.2.

The second finding supported the ANLS hypothesis construct of two metabolic pathways (oxidative and nonoxidative) that coexist, are dissociable, and serve different purposes in maintaining neuronal functions during visual stimulation. Oxidative metabolism is predominantly neuronal and supports ATP production for the release of neurotransmitters, whereas nonoxidative metabolism occurs mainly in astrocytes and supports Glu–Gln recycling and lactogenesis-mediated hyperemia.

The third finding was consistent with the ANLS prediction that some lactate produced by anaerobic glycolysis in astrocytes is effluxed into the circulation. The increased lactate:pyruvate and NADH:NAD$^+$ ratios in blood then activate the nitric oxide signaling pathway, to increase local CBF (27, 29, 31). However, astrocyte-mediated glycolytic metabolism may not be the sole mechanism to elicit this CBF response. Local CBF increase also has been proposed via Ca^{2+}, K^+, and adenosine signaling pathways (29, 32, 33).

Although findings from (20) support current neurophysiological hypotheses, such as the ANLS hypothesis, theories of neurovascular and neurometabolic mechanisms continue to evolve (34). Some aspects of the ANLS hypothesis remain controversial. For example, whether the lactate transferred to neurons as a fuel substrate is from astrocytic or neuronal activity (30), and whether lactate is the preferential substrate of neurons for neurotransmission-related energy needs are still under debate. (See review in (35)). Finally, whether J_{ATP} is constant during continuous stimulation, as this study assumes, remains open. Further investigations are needed to resolve these issues.

In summary, the ANLS model offers a more explicit and comprehensive explanation of the interplay of neuronal activation, metabolism, and hemodynamics that is based on the discovery of the CBF–$CMRO_2$ uncoupling phenomenon.

3. Conclusion

Over the past century, the visual cortex has played a significant role in revealing the fundamental relationship among brain activity, metabolism, and hemodynamics. The development of PET imaging facilitated the investigations and led to the discovery of flow–metabolism uncoupling, the development of fMRI BOLD techniques, and the evolution of the physiological interpretation. These revolutionized changes enable us to better understand the metabolic physiology of brain activity, giving us the bases to predict metabolic physiology in neurological disorders, including stroke or Alzheimer's disease.

Author details

Ai-Ling Lin and Peter T. Fox
Research Imaging Institute, University of Texas Health Science Center, San Antonio, TX, USA

Jia-Hong Gao
Brain Research Imaging Center, University of Chicago, Chicago, IL, USA

4. References

[1] Mosso A. *Ueber den Kreislauf des Blutes im menschlichen Gehirn*. Leipzig: Verlag von Veit. 1881.

[2] Fox PT, Raichle ME, Mintun MA, Dence C. Nonoxidative glucose consumption during focal physiologic neural activity. Science. 1988;241(4864):462-4. Epub 1988/07/22.

[3] Ogawa S, Menon RS, Tank DW, Kim SG, Merkle H, Ellermann JM, et al. Functional brain mapping by blood oxygenation level-dependent contrast magnetic resonance imaging. A comparison of signal characteristics with a biophysical model. Biophys J. 1993;64(3):803-12. Epub 1993/03/01.

[4] Ogawa S, Tank DW, Menon R, Ellermann JM, Kim SG, Merkle H, et al. Intrinsic signal changes accompanying sensory stimulation: functional brain mapping with magnetic resonance imaging. Proc Natl Acad Sci U S A. 1992;89(13):5951-5. Epub 1992/07/01.

[5] Patrizi ML. Primi esperimenti intorno all'influenza della musica sulla circolazione del sangue nel cervello dell'uomo. Rivista Musicale Italiana. 1896;3:275-94.

[6] Roy CS, Sherrington CS. On the Regulation of the Blood-supply of the Brain. J Physiol. 1890;11(1-2):85-158 17. Epub 1890/01/01.

[7] Fulton JF. Observation upon the vascularity of the human occipital lobe during visual activity. Brain. 1928;51:310-20.

[8] Fox PT, Raichle ME. Stimulus rate dependence of regional cerebral blood flow in human striate cortex, demonstrated by positron emission tomography. J Neurophysiol. 1984;51(5):1109-20. Epub 1984/05/01.

[9] Fox PT, Raichle ME. Stimulus rate determines regional brain blood flow in striate cortex. Ann Neurol. 1985;17(3):303-5. Epub 1985/03/01.

[10] Phelps ME, Mazziotta JC. Positron emission tomography: human brain function and biochemistry. Science. 1985;228(4701):799-809. Epub 1985/05/17.

[11] Prichard J, Rothman D, Novotny E, Petroff O, Kuwabara T, Avison M, et al. Lactate rise detected by 1H NMR in human visual cortex during physiologic stimulation. Proc Natl Acad Sci U S A. 1991;88(13):5829-31. Epub 1991/07/01.

[12] Frahm J, Kruger G, Merboldt KD, Kleinschmidt A. Dynamic uncoupling and recoupling of perfusion and oxidative metabolism during focal brain activation in man. Magn Reson Med. 1996;35(2):143-8. Epub 1996/02/01.

[13] Vafaee MS, Gjedde A. Model of blood-brain transfer of oxygen explains nonlinear flow-metabolism coupling during stimulation of visual cortex. J Cereb Blood Flow Metab. 2000;20(4):747-54. Epub 2000/04/25.

[14] Mintun MA, Vlassenko AG, Shulman GL, Snyder AZ. Time-related increase of oxygen utilization in continuously activated human visual cortex. Neuroimage. 2002;16(2):531-7. Epub 2002/05/29.

[15] Kwong KK, Belliveau JW, Chesler DA, Goldberg IE, Weisskoff RM, Poncelet BP, et al. Dynamic magnetic resonance imaging of human brain activity during primary sensory stimulation. Proc Natl Acad Sci U S A. 1992;89(12):5675-9. Epub 1992/06/15.

[16] Detre JA, Leigh JS, Williams DS, Koretsky AP. Perfusion imaging. Magn Reson Med. 1992;23(1):37-45. Epub 1992/01/01.

[17] Davis TL, Kwong KK, Weisskoff RM, Rosen BR. Calibrated functional MRI: mapping the dynamics of oxidative metabolism. Proc Natl Acad Sci U S A. 1998;95(4):1834-9. Epub 1998/03/21.

[18] Gusnard DA, Raichle ME. Searching for a baseline: functional imaging and the resting human brain. Nat Rev Neurosci. 2001;2(10):685-94. Epub 2001/10/05.

[19] Hoge RD, Atkinson J, Gill B, Crelier GR, Marrett S, Pike GB. Linear coupling between cerebral blood flow and oxygen consumption in activated human cortex. Proc Natl Acad Sci U S A. 1999;96(16):9403-8. Epub 1999/08/04.

[20] Lin AL, Fox PT, Hardies J, Duong TQ, Gao JH. Nonlinear coupling between cerebral blood flow, oxygen consumption, and ATP production in human visual cortex. Proc Natl Acad Sci U S A. 2010;107(18):8446-51. Epub 2010/04/21.

[21] Chen W, Zhu XH, Gruetter R, Seaquist ER, Adriany G, Ugurbil K. Study of tricarboxylic acid cycle flux changes in human visual cortex during hemifield visual stimulation using (1)H-[(13)C] MRS and fMRI. Magn Reson Med. 2001;45(3):349-55. Epub 2001/03/10.

[22] Kim SG, Rostrup E, Larsson HB, Ogawa S, Paulson OB. Determination of relative CMRO2 from CBF and BOLD changes: significant increase of oxygen consumption rate during visual stimulation. Magn Reson Med. 1999;41(6):1152-61. Epub 1999/06/17.

[23] Pellerin L, Magistretti PJ. Glutamate uptake into astrocytes stimulates aerobic glycolysis: a mechanism coupling neuronal activity to glucose utilization. Proc Natl Acad Sci U S A. 1994;91(22):10625-9. Epub 1994/10/25.

[24] Belanger M, Allaman I, Magistretti PJ. Brain energy metabolism: focus on astrocyte-neuron metabolic cooperation. Cell Metab. 2011;14(6):724-38. Epub 2011/12/14.

[25] Brand MD. The efficiency and plasticity of mitochondrial energy transduction. Biochem Soc Trans. 2005;33(Pt 5):897-904. Epub 2005/10/26.

[26] Hyder F, Patel AB, Gjedde A, Rothman DL, Behar KL, Shulman RG. Neuronal-glial glucose oxidation and glutamatergic-GABAergic function. J Cereb Blood Flow Metab. 2006;26(7):865-77. Epub 2006/01/13.

[27] Mintun MA, Vlassenko AG, Rundle MM, Raichle ME. Increased lactate/pyruvate ratio augments blood flow in physiologically activated human brain. Proc Natl Acad Sci U S A. 2004;101(2):659-64. Epub 2004/01/06.

[28] Lin AL, Fox PT, Yang Y, Lu H, Tan LH, Gao JH. Time-dependent correlation of cerebral blood flow with oxygen metabolism in activated human visual cortex as measured by fMRI. NeuroImage. 2009;44(1):16-22. Epub 2008/09/23.

[29] Vlassenko AG, Rundle MM, Raichle ME, Mintun MA. Regulation of blood flow in activated human brain by cytosolic NADH/NAD+ ratio. Proc Natl Acad Sci U S A. 2006;103(6):1964-9. Epub 2006/02/01.

[30] Gjedde A, Marrett S. Glycolysis in neurons, not astrocytes, delays oxidative metabolism of human visual cortex during sustained checkerboard stimulation in vivo. J Cereb Blood Flow Metab. 2001;21(12):1384-92. Epub 2001/12/12.

[31] Mangia S, Tkac I, Gruetter R, Van de Moortele PF, Maraviglia B, Ugurbil K. Sustained neuronal activation raises oxidative metabolism to a new steady-state level: evidence from 1H NMR spectroscopy in the human visual cortex. J Cereb Blood Flow Metab. 2007;27(5):1055-63. Epub 2006/10/13.

[32] Takano T, Tian GF, Peng W, Lou N, Libionka W, Han X, et al. Astrocyte-mediated control of cerebral blood flow. Nat Neurosci. 2006;9(2):260-7. Epub 2006/01/03.

[33] Haddy FJ, Vanhoutte PM, Feletou M. Role of potassium in regulating blood flow and blood pressure. Am J Physiol Regul Integr Comp Physiol. 2006;290(3):R546-52. Epub 2006/02/10.

[34] Attwell D, Buchan AM, Charpak S, Lauritzen M, Macvicar BA, Newman EA. Glial and neuronal control of brain blood flow. Nature. 2010;468(7321):232-43. Epub 2010/11/12.

[35] Mangia S, Giove F, Tkac I, Logothetis NK, Henry PG, Olman CA, et al. Metabolic and hemodynamic events after changes in neuronal activity: current hypotheses, theoretical predictions and in vivo NMR experimental findings. J Cereb Blood Flow Metab. 2009;29(3):441-63. Epub 2008/11/13.

IntechOpen